

Correlation functions of the quantum sine-Gordon model in and out of equilibrium

I. Kukuljan,¹ S. Sotiriadis,¹ and G. Takacs^{2,3}

¹University of Ljubljana, Faculty of Mathematics and Physics, Jadranska ulica 19, SI-1000 Ljubljana, Slovenia

²BME ‘‘Momentum’’ Statistical Field Theory Research Group, H-1117 Budapest, Budafoki út 8, Hungary

³BME Department of Theoretical Physics, H-1117 Budapest, Budafoki út 8, Hungary

(Dated: June 10, 2022)

Complete information on the equilibrium behaviour and dynamics of Quantum Field Theory (QFT) is provided by the field correlation functions. However their theoretical calculation is a challenging problem, even for exactly solvable models. This has recently become an experimentally relevant problem, due to progress in cold-atom experiments simulating QFT models and directly measuring higher order correlations. We compute correlation functions of the quantum sine-Gordon model, a prototype integrable model of central interest from both theoretical and experimental point of view. Building upon the so-called Truncated Conformal Space Approach, we numerically construct higher order correlations in a system of finite size in various physical states of experimental relevance, both in and out of equilibrium. We measure deviations from Gaussianity due to the presence of interaction and analyse their dependence on temperature, explaining the experimentally observed crossover between Gaussian and non-Gaussian regimes. We find that correlations of excited states are markedly different from the thermal case, which can be explained by integrability of the system. We also study dynamics after a quench, observing the effects of the interaction on the time evolution of correlation functions, their spatial dependence and a global measure of non-Gaussianity.

PACS numbers: 03.70.+k, 11.55.Ds, 67.85.-d, 03.75.Hh, 03.75.Kk

Introduction. - Correlation functions provide a complete and practical description of a physical system. Any observable can be expressed directly in their terms and they can be used to deduce information about the spectrum of quasiparticles and their collisions [1]. In particular, knowledge of higher order correlation functions is necessary in order to distinguish the ground or thermal states of an interacting from those of a non-interacting system: while such states are Gaussian for non-interacting systems, that is their cumulants (a.k.a. connected correlation functions) of order higher than two vanish, those of interacting systems are generally non-Gaussian.

Recent developments in atom interferometry of ultracold atom experiments have made possible the measurement of correlation functions of any order, in both spatial and temporal resolution [2, 3]. Ultracold atoms used in these experiments can be confined in elongated potential traps, so that they form essentially one-dimensional (1d) quantum gases [4]. Such gases are gapless systems, described in terms of their density and phase fields by means of *Luttinger liquid* theory [5, 6]. By splitting the trap in the transverse direction to form two parallel nearby traps however, the tunneling between the two traps gives rise to *Josephson junction* physics [7]. This induces an effective self-interaction on the phase difference between the two condensates, such that its low energy physics is described by the *sine-Gordon* model (SGM) [8–10], a prominent example of a strongly-correlated quantum field theory. However it is still unclear to what extent this description is valid in out of equilibrium settings [11], like after a *quantum quench*, where an abrupt change of the interaction creates excitations of arbitrarily high

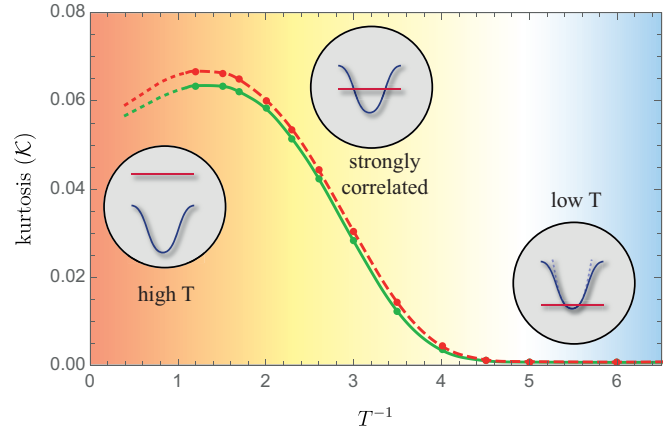


Figure 1. Kurtosis, measure of non-Gaussianity of thermal states as a function of the inverse temperature T^{-1} for interactions $\Delta \equiv \beta^2/(8\pi) = 1/100$ (red line) and $1/18$ (green line). Deviations from Gaussianity increase with temperature up to a maximum at $T \sim 1$ (in units of soliton mass M) and decrease at higher T . Our method describes accurately the low and intermediate temperature regime $T \gtrsim 1$. Insets illustrate the excitation level in units of the potential height as defined in [35].

energy.

The SGM is one of the most studied physical models, as it describes 2d classical (XY model) [12] and 1d quantum systems (e.g. spin chains). It exhibits rich physics such as *solitons* and anti-solitons, as well as their bound states, so-called *breathers*, and it has a topological *Berezinskii-Kosterlitz-Thouless* phase transition.

Both the classical and the quantum versions are in-

tegrable [13, 14], i.e. possess an infinite number of local conserved quantities allowing exact solution. Despite this fact, the analytical calculation of correlation functions for this model is a highly non-trivial task and no theoretical results are available for higher order correlations. For this reason the development of numerical methods is of utmost importance, both for verification of analytical predictions and for comparison with experimental data in order to check how close to the SGM the actual experimental system is.

In this Letter we present an application of the so-called “*Truncated Conformal Space Approach*” (TCSA) [15] for the calculation of SGM correlation functions in finite systems. The TCSA uses the *Renormalisation Group* (RG) *fixed point* of the system under consideration, as a reference basis for an efficient numerical diagonalisation of the Hamiltonian [16–18]. It works perfectly in many cases where perturbation theory fails and is suitable for the study of continuous models in 1d and even higher dimensions [19], unlike DMRG methods that work principally for lattice 1d models.

While this approach has been used extensively for the study of the SGM [18, 20, 21], the calculation of correlation functions has not been achieved until now. In the present work we perform this task for a convenient choice of boundary conditions, the Dirichlet type. We validate our numerics comparing with the known mass spectrum [13, 22] and single point observables of the SGM [23, 24]. We then calculate two point (2-p) and four point (4-p) correlation functions of the bosonic field ϕ in coordinate space for different values of the interaction, system size and temperature. We study a variety of different settings: ground states, thermal equilibrium and excited states, as well as quench dynamics, focusing on measures of the non-Gaussianity of the state due to the presence of interactions and performing spectral analysis. In contrast to other approximations for the analysis of equilibrium [25–27] or quench dynamics [28–34] our approach allows to compute multi-point correlations and study the full quantum many-body dynamics.

The sine-Gordon model. - The SGM is a relativistically invariant model of an interacting bosonic field ϕ , described by the Hamiltonian

$$H_{SGM} = \int \left(\frac{1}{2}(\partial_t \phi)^2 + \frac{1}{2}(\partial_x \phi)^2 - \frac{m^2}{\beta^2} \cos \beta \phi \right) dx$$

For $\Delta \equiv \frac{\beta^2}{8\pi} > 1$ it is gapless, as the $\cos \beta \phi$ “potential energy” term is an irrelevant perturbation of the free massless boson Hamiltonian $H_{FB} = \frac{1}{2} \int (\partial_\mu \phi)^2 dx$ and the system behaves as a freely fluctuating field. For $\Delta < 1$ instead the interaction is relevant and the system is macroscopically described by a field locked in one of the cosine minima and becomes gapped. Its spectrum in the gapped regime consists of soliton and antisoliton excitations of mass M , as well as breathers, the number of which is

determined by the value of its interaction parameter β : the smaller the value of β , the more breather modes are present [35]. Based merely on integrability and relativistic invariance [36], the exact particle masses [13, 22], scattering matrix [37], ground state expectation values [23] and matrix elements of local observables (*form factors*) [38] are known. Despite its exceptional solvability properties however, only limited information is available about its correlation functions. Integrability allows to compute single point expectation values in finite size and thermal [24, 39, 40] or out-of-equilibrium systems [28, 40–42] and the infinite volume ground state 2-p function [43]. However there are no results available for multi-point observables in thermal or out-of-equilibrium contexts with full QFT dynamics.

TCSA. - The TCSA, introduced in [15] and later applied to the SGM [18, 20, 21], is based on the idea of using the eigenstate basis of a known reference Hamiltonian H_0 , truncated up to a specified maximum energy cutoff E_{cutoff} , to construct the ground and excited states of a different Hamiltonian $H_0 + V$, with V having known matrix elements in the basis of H_0 . The main idea of TCSA and the reason for its success is to choose as reference Hamiltonian H_0 the critical model associated with the UV fixed point of the RG flow that describes the model under consideration. *Conformal Field Theory* (CFT) [44] provides all algebraic tools needed in order to construct the eigenstates and energy spectrum of H_0 , as well as the matrix elements of V in this basis. Diagonalisation of $H_0 + V$ in the truncated Hilbert space reduces then to a finite dimensional matrix problem. The TCSA is ideal for computing the energy spectrum of $H_0 + V$ efficiently, it can be used to capture effects beyond perturbation theory and is especially suited for relevant operators V , integrable or not, being useful also for marginal and irrelevant ones. For the SGM, H_0 is the free massless boson Hamiltonian and the perturbing operator $V \propto \int dx \cos \beta \phi$ corresponds to the spatial integral of the sum of two so-called “*vertex operators*” $\exp(\pm i\beta\phi)$. Here we consider a finite system of size L with Dirichlet boundary conditions $\phi(0) = \phi(L) = 0$, which preserve integrability [45] and induce well understood changes to the energy spectrum [46, 47]. This choice of boundary conditions significantly simplifies the computation of ϕ correlations with TCSA, since the only relevant sector of the conformal basis is the zero topological charge sector [35].

Correlations in equilibrium states. - We start our analysis with equilibrium states: ground and thermal states. Figs. 2 and 3 show typical plots of 2-p and 4-p functions in ground and thermal states of the SGM at interaction $\Delta = 1/18 \approx 0.055$, which is in the highly attractive regime similarly to the experimentally realised system, and well inside the window where our numerics can reliably produce a large part of the excitation spectrum.

The plots can be compared with those of the free mass-

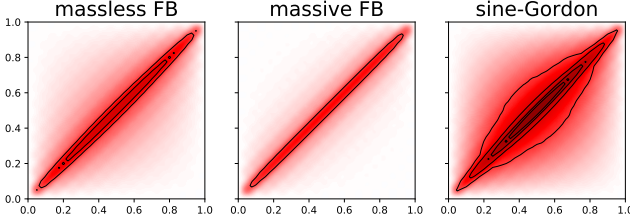


Figure 2. Density plots of 2-p correlations $G^{(2)}(x_1, x_2)$ on the ground state of the SGM in a box (right) in comparison with those of the massless (left) and massive (middle) free boson case (interaction: $\Delta = 1/18$, system size: $L = 25$, mass of the free case chosen equal to first breather mass of the SGM).

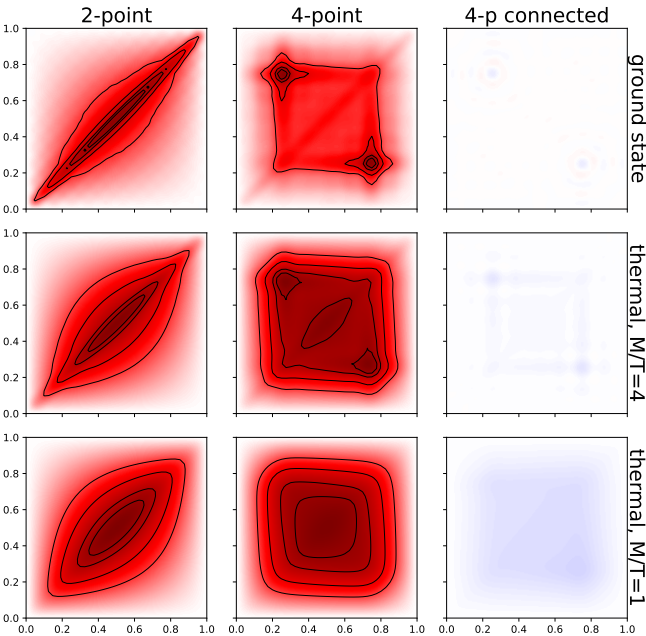


Figure 3. Density plots of 2-p correlations $G^{(2)}(x_1, x_2)$ and 4-p full and connected correlations $G^{(4)}(x_1, x_2, \frac{1}{4}L, \frac{3}{4}L)$ for the ground and two thermal states ($\Delta = 1/18$, $L = 25$, $T = 0, 0.25, 1$ in units M).

less or free massive case with mass equal to the lowest breather mass (Fig 2): switching on the interaction results in dramatic growth of ground state correlations that are also longer in range than in the free case. At the same time 4-p connected correlations appear, signalling the non-Gaussianity of the state, even though their magnitude in ground states is relatively small in comparison with the 2-p correlations. Larger deviations from Gaussianity are seen in thermal or excited states. This behaviour is easily explained by a semiclassical argument. The ground state energy is close to the bottom of the cosine potential energy, where it can be approximated by a parabola quite well. In contrast, the presence of excitations in thermal states allows us to explore the non-

parabolic shape of the potential energy. At even larger temperature, correlations are dominated by excitations with energy much higher than the potential energy, which are essentially free massless bosonic modes and so non-Gaussianity is suppressed.

This is demonstrated in Fig. 1 which plots the *kurtosis* \mathcal{K} (ratio of connected over disconnected 4-p correlations integrated over all space, c.f. [35]) as a function of the temperature: its maximum value is observed at temperatures comparable to the height of the cosine potential i.e. $T \sim 1$. This thermal effect is precisely what gives rise to the experimental observation of three different regimes of the SGM [2]: free massless phonons (high T), coexistence of interacting massive phonons and solitons (intermediate T), and free massive phonons (low T). Notice also how increasing the temperature results in correlations being less concentrated along the diagonal (Fig. 3).

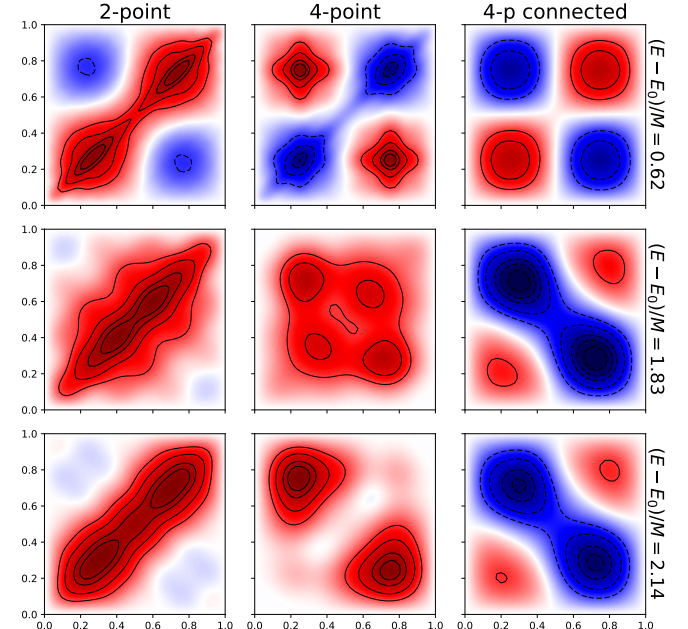


Figure 4. Density plots of 2-p, 4-p full and connected correlations for some low-energy excited states (energy unit: M).

While ground and thermal states exhibit a rather simple pattern, characterised by decay of correlations with separation distance, excited states display much richer structure, as can be seen in Fig. 4. The strong qualitative difference between excited and thermal state correlations may be seen as a violation of the *Eigenstate Thermalisation Hypothesis* [48–50] for the SGM: due to its integrability, a typical eigenstate exhibits local characteristics dramatically different from those of a thermal state at the same energy level. The patterns in Fig. 4 are similar to those observed in [2], suggesting that the experimentally realised states are closer to low energy excited states rather than thermal states of the SGM.

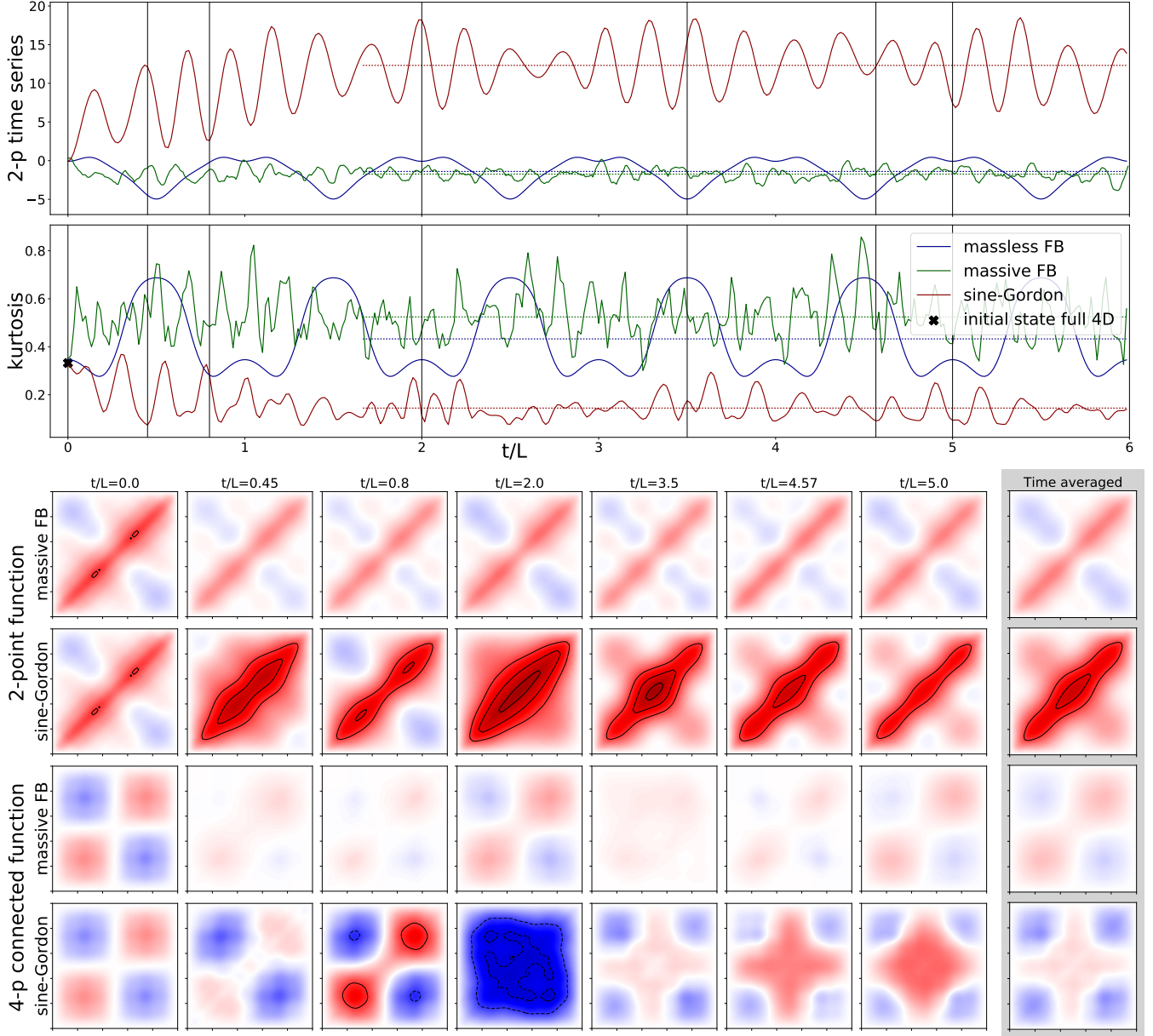


Figure 5. Time evolution of 2-p correlations $G^{(2)}(L/3, 2L/3; t)$ (top), kurtosis (middle) and spatial density plots of 2-p correlations $G^{(2)}(x_1, x_2; t)$ and 4-p correlations $G^{(4)}(x_1, x_2, L/4, 3L/4; t)$ at various times t (bottom four rows) after a quench starting from an excited state of the SGM (pre-quench interaction: $\Delta_0 = 1/18$, post-quench interaction: $\Delta = 1/8$, initial state energy $\sim 0.73M$ above ground state, corresponding to 50% of the height of the cosine potential, $L = 30/M$). Correlations under massless and massive free boson dynamics (with mass matched to that of the first breather of the SGM) are plotted together for comparison.

Correlations in out-of-equilibrium states. - We now turn our attention to out-of-equilibrium settings. We consider the dynamics after a quench where the initial state is an excited state of the SGM for some value of the interaction $\Delta_0 = 1/18$ and the time evolution corresponds to another value $\Delta = 1/8$. Using an excited rather than ground or thermal state as initial state results in a higher density of post-quench excitations and

in more interesting dynamics beyond the regime of validity of low density or semiclassical approximations [35]. Fig. 5 shows the time evolution of 2-p function at two fixed points and of the kurtosis, as well as snapshots of the spatial dependence of 2-p and 4-p functions at various times and after time averaging. For comparison we present also the time evolution of the same initial state under free massless or massive dynamics.

We observe the strongly oscillatory form of dynamics in all three cases. However, despite initiating from the same state, the three types of dynamics result in different oscillation frequency, time averages and amplitude of fluctuations about the average. The free massless case is exceptional in that the dynamics is purely periodic with revival period $t_R = L$ since, because of their linear dispersion, all modes have energies that are integer multiples of $2\pi/L$. In the free massive case exact periodicity is lost, because particle velocity depends now on momentum. Instead, we observe phase oscillations with frequencies dominated by the particle mass. Dynamics under the SGM are characterised by multi-frequency oscillations [9] and a general amplification of the initial correlations compared to the free case.

The dynamics of kurtosis reveals also another interesting property. In contrast to the free cases where it exhibits strong fluctuations about the time average and passes frequently close to its initial value, the SGM dynamics are characterised by a long plateau with relatively small fluctuations about the time average, different from its initial value. This observation points to the concept of *equilibration on average* [51–53] which applies to finite systems. Note that spatially integrated local observables like the kurtosis are essentially global measures of correlations. The difference between free and interacting dynamics of the kurtosis can be attributed to the fact that in the free case the ϕ field is related in a simple linear way to the system's diagonal modes. On the contrary, in the interacting case its mode (or form factor) expansion is intrinsically far more complicated, resulting in efficient dephasing even for such a global quantity.

Discussion. - We have demonstrated that the truncated Hamiltonian approach can be efficiently applied to compute multi-point correlation functions both in and out of equilibrium, which also allows access to non-Gaussianity measures, such as the kurtosis. In the case of sine-Gordon model we observe that quench dynamics changes the spatial pattern of the connected 4-p correlations substantially, which is in marked contrast with the free case and can be seen as a non-trivial effect of interactions. We also note that the excited state connected 4-p correlations are significantly different from the thermal ones, which can be understood on the basis of integrability.

The work was partially supported by the Advanced Grant of European Research Council (ERC) 694544 – OMNES, by the Slovenian Research Agency under grants N1-0025, N1-0055 and P1-0044, as well as by the National Research Development and Innovation Office of Hungary within the Quantum Technology National Excellence Program (Project No. 2017-1.2.1-NKP-2017-00001) and under OTKA grant No. SNN118028.

- [1] S. Weinberg, *The Quantum Theory of Fields*. Cambridge University Press, 1995.
- [2] T. Schweigler, V. Kasper, S. Erne, I. Mazets, B. Rauer, F. Cataldini, T. Langen, T. Gasenzer, J. Berges, and J. Schmiedmayer, “Experimental characterization of a quantum many-body system via higher-order correlations,” *Nature* **545** no. 7654, (2017) 323–326.
- [3] T. Langen, S. Erne, R. Geiger, B. Rauer, T. Schweigler, M. Kuhnert, W. Rohringer, I. E. Mazets, T. Gasenzer, and J. Schmiedmayer, “Experimental observation of a generalized Gibbs ensemble,” *Science* **348** no. 6231, (2015) 207–211.
- [4] M. A. Cazalilla, R. Citro, T. Giamarchi, E. Orignac, and M. Rigol, “One dimensional bosons: From condensed matter systems to ultracold gases,” *Reviews of Modern Physics* **83** no. 4, (2011) 1405–1466.
- [5] F. D. M. Haldane, “‘Luttinger liquid theory’ of one-dimensional quantum fluids. I. Properties of the Luttinger model and their extension to the general 1D interacting spinless Fermi gas,” *Journal of Physics C: Solid State Physics* **14** no. 19, (1981) 2585–2609.
- [6] V. Mastropietro and D. C. Mattis, *Luttinger Model: The First 50 Years and Some New Directions (Series on Directions in Condensed Matter Physics)*. World Scientific Publishing Company, 2013.
- [7] F. S. Cataliotti, S. Burger, C. Fort, P. Maddaloni, F. Minardi, A. Trombettoni, A. Smerzi, and M. Inguscio, “Josephson Junction Arrays with Bose-Einstein Condensates,” *Science* **293** no. 5531, (2001) 843–846.
- [8] V. Gritsev, E. Altman, E. Demler, and A. Polkovnikov, “Full quantum distribution of contrast in interference experiments between interacting one-dimensional Bose liquids,” *Nature Physics* **2** no. 10, (2006) 705–709.
- [9] V. Gritsev, E. Demler, M. Lukin, and A. Polkovnikov, “Spectroscopy of Collective Excitations in Interacting Low-Dimensional Many-Body Systems Using Quench Dynamics,” *Physical Review Letters* **99** no. 20, (2007) .
- [10] V. Gritsev, A. Polkovnikov, and E. Demler, “Linear response theory for a pair of coupled one-dimensional condensates of interacting atoms,” *Physical Review B* **75** no. 17, (2007) .
- [11] M. Pigneur, T. Berrada, M. Bonneau, T. Schumm, E. Demler, and J. Schmiedmayer, “Relaxation to a Phase-locked Equilibrium State in a One-dimensional Bosonic Josephson Junction,” *arxiv:1711.06635* (2017) . <https://arxiv.org/abs/1711.06635>.
- [12] D. J. Amit, Y. Y. Goldschmidt, and S. Grinstein, “Renormalisation group analysis of the phase transition in the 2D Coulomb gas, Sine-Gordon theory and XY-model,” *Journal of Physics A: Mathematical and General* **13** no. 2, (1980) 585–620.
- [13] V. E. Korepin and L. D. Faddeev, “Quantization of solitons,” *Theoretical and Mathematical Physics* **25** no. 2, (1975) 1039–1049.
- [14] L. Faddeev and V. Korepin, “Quantum theory of solitons,” *Physics Reports* **42** no. 1, (1978) 1–87.
- [15] V. P. Yurov and A. B. Zamolodchikov, “Truncated Conformal Space Approach to scaling Lee-Yang model,” *International Journal of Modern Physics A* **05** no. 16, (1990) 3221–3245.

[16] M. Lässig, G. Mussardo, and J. L. Cardy, “The scaling region of the tricritical Ising model in two dimensions,” *Nuclear Physics B* **348** no. 3, (1991) 591–618.

[17] V. Yurov and A. Zamolodchikov, “Truncated-fermionic-space approach to the critical 2d Ising model with magnetic field,” *International Journal of Modern Physics A* **06** no. 25, (1991) 4557–4578.

[18] G. Feverati, F. Ravanini, and G. Takács, “Truncated conformal space at $c = 1$, nonlinear integral equation and quantization rules for multi-soliton states,” *Physics Letters B* **430** no. 3-4, (1998) 264–273.

[19] M. Hogervorst, S. Rychkov, and B. C. van Rees, “Truncated conformal space approach in d dimensions: A cheap alternative to lattice field theory?,” *Physical Review D* **91** no. 2, (2015) .

[20] G. Feverati, F. Ravanini, and G. Takács, “Non-linear integral equation and finite volume spectrum of sine-gordon theory,” *Nuclear Physics B* **540** no. 3, (1999) 543–586.

[21] G. Fehér and G. Takács, “Sine-Gordon form factors in finite volume,” *Nuclear Physics B* **852** no. 2, (2011) 441–467.

[22] R. F. Dashen, B. Hasslacher, and A. Neveu, “Particle spectrum in model field theories from semiclassical functional integral techniques,” *Physical Review D* **11** no. 12, (1975) 3424–3450.

[23] S. Lukyanov and A. Zamolodchikov, “Exact expectation values of local fields in the quantum sine-Gordon model,” *Nuclear Physics B* **493** no. 3, (1997) 571–587.

[24] F. Buccheri and G. Takács, “Finite temperature one-point functions in non-diagonal integrable field theories: the sine-Gordon model,” *Journal of High Energy Physics* **2014** no. 3, (2014) .

[25] K. Damle and S. Sachdev, “Universal Relaxational Dynamics of Gapped One-Dimensional Models in the Quantum Sine-Gordon Universality Class,” *Physical Review Letters* **95** no. 18, (2005) .

[26] S. Beck, I. E. Mazets, and T. Schweigler, “A Non-Perturbative Method to compute Thermal Correlations in One-Dimensional Systems,” *arxiv:1712.01190* (2017) .
<https://arxiv.org/abs/1712.01190>.

[27] S. Beck, I. E. Mazets, and T. Schweigler, “Non-perturbative method to compute thermal correlations in one-dimensional systems: A detailed analysis,” *arxiv:1802.06610* (2018) .
<https://arxiv.org/abs/1802.06610>.

[28] B. Bertini, D. Schuricht, and F. H. L. Essler, “Quantum quench in the sine-Gordon model,” *Journal of Statistical Mechanics: Theory and Experiment* **2014** no. 10, (2014) P10035.

[29] L. Foini and T. Giamarchi, “Nonequilibrium dynamics of coupled Luttinger liquids,” *Physical Review A* **91** no. 2, (2015) .

[30] L. Foini and T. Giamarchi, “Relaxation dynamics of two coherently coupled one-dimensional bosonic gases,” *The European Physical Journal Special Topics* **226** no. 12, (2017) 2763–2774.

[31] L. Foini, A. Gambassi, R. Konik, and L. F. Cugliandolo, “Measuring effective temperatures in a generalized Gibbs ensemble,” *Physical Review E* **95** no. 5, (2017) .

[32] J. D. Nardis, M. Panfil, A. Gambassi, R. Konik, L. Cugliandolo, and L. Foini, “Probing non-thermal density fluctuations in the one-dimensional Bose gas,” *SciPost Physics* **3** no. 3, (2017) .

[33] M. Kormos and G. Zaránd, “Quantum quenches in the sine-Gordon model: A semiclassical approach,” *Physical Review E* **93** no. 6, (2016) .

[34] C. P. Moca, M. Kormos, and G. Zaránd, “Hybrid Semiclassical Theory of Quantum Quenches in One-Dimensional Systems,” *Physical Review Letters* **119** no. 10, (2017) .

[35] See Supplementary Material for details.

[36] A. B. Zamolodchikov and A. B. Zamolodchikov, “Factorized S-matrices in two dimensions as the exact solutions of certain relativistic quantum field theory models,” *Annals of Physics* **120** no. 2, (1979) 253–291.

[37] A. B. Zamolodchikov, “Exact two-particle S-matrix of quantum sine-Gordon solitons,” *Communications in Mathematical Physics* **55** no. 2, (1977) 183–186.

[38] F. A. Smirnov, *Form Factors in Completely Integrable Models of Quantum Field Theory (Advanced Series in Mathematical Physics)*. World Scientific Pub Co Inc, 1992.

[39] A. LeClair and G. Mussardo, “Finite temperature correlation functions in integrable QFT,” *Nuclear Physics B* **552** no. 3, (1999) 624–642.

[40] B. Pozsgay, “Mean values of local operators in highly excited bethe states,” *Journal of Statistical Mechanics: Theory and Experiment* **2011** no. 01, (2011) P01011.

[41] D. Fioretto and G. Mussardo, “Quantum quenches in integrable field theories,” *New Journal of Physics* **12** no. 5, (2010) 055015.

[42] A. C. Cubero and D. Schuricht, “Quantum quench in the attractive regime of the sine-Gordon model,” *Journal of Statistical Mechanics: Theory and Experiment* **2017** no. 10, (2017) 103106.

[43] F. H. Essler and R. M. Konik, “Applications of Massive Integrable Quantum Field Theories to Problems in Condensed Matter Physics,” in *From Fields to Strings: Circumnavigating Theoretical Physics*, pp. 684–830. World Scientific, 2005.

[44] P. D. Francesco, P. Mathieu, and D. Sénéchal, *Conformal Field Theory*. Springer New York, 1997.

[45] S. Ghoshal and A. Zamolodchikov, “Boundary S-Matrix and Boundary State in Two-Dimensional Integrable Quantum Field Theory,” *International Journal of Modern Physics A* **09** no. 21, (1994) 3841–3885.

[46] Z. Bajnok, L. Palla, and G. Takács, “Boundary states and finite size effects in sine-Gordon model with Neumann boundary condition,” *Nuclear Physics B* **614** no. 3, (2001) 405–448.

[47] Z. Bajnok, L. Palla, and G. Takács, “Finite size effects in boundary sine-Gordon theory,” *Nuclear Physics B* **622** no. 3, (2002) 565–592.

[48] J. M. Deutsch, “Quantum statistical mechanics in a closed system,” *Physical Review A* **43** no. 4, (1991) 2046–2049.

[49] M. Srednicki, “Chaos and quantum thermalization,” *Physical Review E* **50** no. 2, (1994) 888–901.

[50] M. Rigol and M. Srednicki, “Alternatives to Eigenstate Thermalization,” *Physical Review Letters* **108** no. 11, (2012) .

[51] J. von Neumann, “Beweis des Ergodensatzes und des H-Theorems in der neuen Mechanik,” *Zeitschrift für Physik* **57** no. 1-2, (1929) 30–70.

[52] J. von Neumann, “Proof of the ergodic theorem and the H-theorem in quantum mechanics,” *The European*

Physical Journal H **35** no. 2, (2010) 201–237.

- [53] C. Gogolin and J. Eisert, “Equilibration, thermalisation, and the emergence of statistical mechanics in closed quantum systems,” *Reports on Progress in Physics* **79** no. 5, (2016) 056001.
- [54] A. B. Zamolodchikov, “Mass scale in the sine-Gordon model and its reductions,” *International Journal of Modern Physics A* **10** no. 08, (1995) 1125–1150.
- [55] A. Klumper, M. T. Batchelor, and P. A. Pearce, “Central charges of the 6- and 19-vertex models with twisted boundary conditions,” *Journal of Physics A: Mathematical and General* **24** no. 13, (1991) 3111–3133.
- [56] C. Destri and H. J. de Vega, “New thermodynamic Bethe ansatz equations without strings,” *Physical Review Letters* **69** no. 16, (1992) 2313–2317.
- [57] S. Ghoshal, “Bound State Boundary S-matrix of the sine-Gordon Model,” *International Journal of Modern Physics A* **09** no. 27, (1994) 4801–4810.

Supplementary Material

The sine-Gordon model spectrum

Mass spectrum - The action of the sine-Gordon model as a perturbed conformal field theory can be written as:

$$\mathcal{S}_{\text{SG}} = \int_{-\infty}^{\infty} dt \int_0^L dx \left[\frac{1}{8\pi} \partial_\nu \varphi(x, t) \partial^\nu \varphi(x, t) + \mu : \cos \left(\frac{\beta}{\sqrt{4\pi}} \varphi(x, t) \right) : \right] \quad (1)$$

where the semicolon denotes normal ordering of the free massless boson modes. The relation between the soliton mass M and the coupling μ is [54]:

$$\mu = \kappa(\xi) M^{2/(\xi+1)}, \quad (2)$$

where the parameter ξ is defined as:

$$\xi = \frac{\beta^2}{8\pi - \beta^2}, \quad (3)$$

and the coupling-mass ratio $\kappa(\xi)$ is [54]:

$$\kappa(\xi) = \frac{2}{\pi} \frac{\Gamma\left(\frac{\xi}{\xi+1}\right)}{\Gamma\left(\frac{1}{\xi+1}\right)} \left[\frac{\sqrt{\pi} \Gamma\left(\frac{\xi+1}{2}\right)}{2 \Gamma\left(\frac{\xi}{2}\right)} \right]^{2/(\xi+1)}. \quad (4)$$

In (1) we have used the rescaled field:

$$\phi =: \frac{1}{\sqrt{4\pi}} \varphi \quad (5)$$

and compactified it on a circle of radius R :

$$\varphi \sim \varphi + 2\pi R, \quad R = \frac{\sqrt{4\pi}}{\beta} = \sqrt{\frac{\xi+1}{2\xi}} \quad (6)$$

to take into account the periodicity of the cosine potential. In the above the length of the system is L and we impose Dirichlet boundary conditions:

$$\varphi(0, t) = \varphi(L, t) = 0 \quad (7)$$

The SGM particle spectrum consists of solitons, anti-solitons and for $\xi < 1$ also breathers, i.e. soliton-antisoliton bound states. For a given ξ , there are $n = 1, 2, \dots < 1/\xi$ breathers with masses:

$$m_n = 2M \sin(n\pi\xi/2) \quad (8)$$

plotted as a function of the interaction $\beta^2/(8\pi) = \xi/(\xi+1)$ in Fig. 6.

Excitation level of states - For any state it is possible to express its excitation level compared to the potential using a single dimensionless quantity. Due to the small β values considered, this can be defined semiclassically. The potential term is then

$$- \int dx \frac{m^2}{\beta^2} \cos \beta \varphi \quad (9)$$

and for small β , the soliton mass is

$$M = \frac{8m}{\beta^2} \quad (10)$$

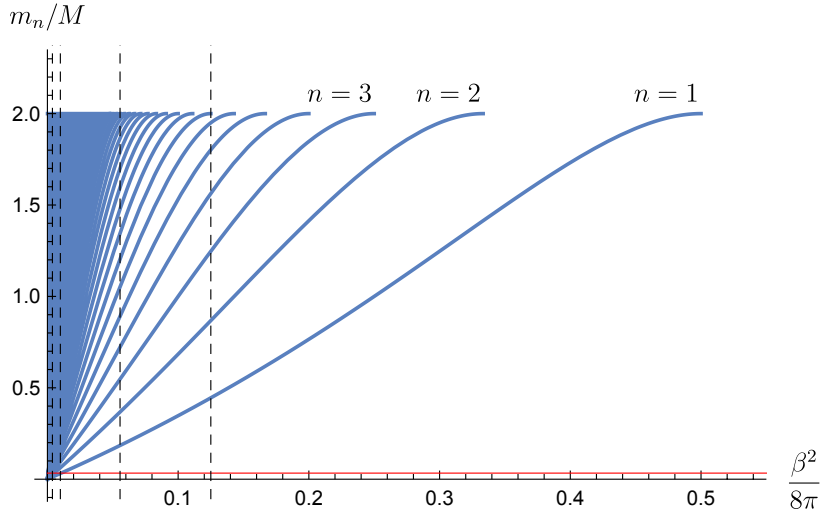


Figure 6. Breather masses m_n in units of soliton mass M as a function of interaction $\beta^2/(8\pi)$. Dashed vertical lines denote the values of interaction used for the numerics: from left to right $\frac{1}{260}$, $\frac{1}{100}$, $\frac{1}{18}$ and $\frac{1}{8}$. The horizontal line denotes the inverse system size $1/L = 1/30$ for comparison: for the largest value of interaction used, the lightest breather mass, which determines the ground state correlation length, is $m_1 L \sim 13$ meaning that the system at ground state is practically close to thermodynamic limit, while for smaller values of interaction finite size effects are quite strong.

Assuming that the energy of the state relative to the ground state is given by χ

$$E - E_0 = \chi M \quad (11)$$

while the potential height in finite volume is

$$\Delta V = \frac{2m^2}{\beta^2} L \quad (12)$$

the relevant ratio is given by

$$\frac{E - E_0}{\Delta V} = \frac{\chi M}{\frac{2m^2}{\beta^2} L} = \frac{4\chi}{mL} \quad (13)$$

where m can be replaced with the first breather mass m_1 in the small β regime.

Truncated Conformal Space Approach for the sine-Gordon correlation functions

In this section we explain the adaptation of the Truncated Conformal Space Approach (TCSA) to compute the correlation functions of the sine-Gordon model on a finite interval. Introducing the vertex operator:

$$V_n(z, \bar{z}) = e^{i \frac{n}{R} \varphi(z, \bar{z})} \quad (14)$$

(using the complex coordinates $z = e^{\frac{\pi}{L}(\tau - ix)}$ and $\bar{z} = e^{\frac{\pi}{L}(\tau + ix)}$), we can write the dimensionless sine-Gordon Hamiltonian as:

$$h_{\text{SG}} := \frac{H_{\text{SG}}}{M} = \frac{H_{\text{FB}}}{M} - \frac{\kappa(\xi)}{2} \left(\frac{\pi}{L} \right)^{2h_\beta - 1} \frac{\pi}{L} \int_0^L dx (V_1(e^{-i\frac{\pi}{L}x}, e^{i\frac{\pi}{L}x}) + V_{-1}(e^{-i\frac{\pi}{L}x}, e^{i\frac{\pi}{L}x})) \quad (15)$$

where

$$H_{\text{FB}} = \frac{1}{8\pi} \int_0^L dx \left[(\partial_t \varphi(x, t))^2 + (\partial_x \varphi(x, t))^2 \right] \quad (16)$$

is the free boson Hamiltonian and $l = ML$ is the dimensionless volume parameter. For the computations presented in this work, we use Dirichlet boundary conditions.

The Hamiltonian (15) is already written in the TCSA form, where the free boson term represents the exactly solvable (conformal) part and the interaction term represents the relevant perturbation. In the following, we would like to discuss the free boson Hilbert space, give the matrix elements of the operators used in the computation and explain how the TCSA simulation is done. Namely, the general idea of the TCSA is to express all the operators appearing in the computation as matrices in the basis of the conformal part and introduce a truncation at certain energy to keep the matrices finite.

Free boson Hilbert space - In this section we briefly recall the structure of the free boson Hilbert space. The general free boson field satisfying Dirichlet boundary conditions takes the form:

$$\varphi(x, \tau) = \varphi_0 - \frac{2\pi}{L} RMx + 2 \sum_{k \neq 0} \frac{a_k}{k} \sin(k \frac{\pi}{L} x) e^{-k \frac{\pi}{L} \tau}. \quad (17)$$

For other boundary conditions (Neumann and periodic), φ_0 is an operator, which is divergent in itself and only its exponential is well defined. In the case of Dirichlet boundary conditions, φ_0 is a complex number corresponding to boundary values of the field. In our case, $\varphi_0 = 0$. The term involving the operator M is interpolating between different vacua of the free boson. In our cases (massless and massive free bosons and sine-Gordon theories) the Hamiltonians do not mix the states between Verma modules descending from the different vacua, so it is sufficient to take a single Verma module. For convenience we choose the module corresponding to the lowest lying vacuum. Therefore the M operator is redundant.

We quantize the field using the following commutation relations:

$$[a_k, a_l] = k \delta_{k+l}. \quad (18)$$

From the vacuum, we can construct descendant states:

$$|\vec{r}\rangle = |r_1, r_2, \dots, r_k, \dots\rangle := \frac{1}{N_{\vec{r}}} \prod_{k=1}^{\infty} a_k^{r_k} |0\rangle, \quad (19)$$

where we have defined

$$a_k |0\rangle \equiv 0, \quad \text{for } k > 0 \quad (20)$$

and the normalization is given by (we have $a_k^\dagger = a_{-k}$):

$$N_{\vec{r}}^2 = \langle 0 | \prod_{k=1}^{\infty} a_k^{r_k} a_{-k}^{r_k} | 0 \rangle = \prod_{k=1}^{\infty} (r_k! k^{r_k}). \quad (21)$$

These states span the Hilbert space:

$$\mathcal{H} := \text{span}(\{|\vec{r}\rangle\}_{\vec{r}}). \quad (22)$$

Matrix elements - To perform the TCSA, we have to compute in the free boson Hilbert space the matrix elements of all operators needed in the computation. This is done by performing the algebra using the commutation relations (18). For a given pair of basis states:

$$|\psi\rangle = |\vec{r}\rangle, \quad (23)$$

$$|\psi'\rangle = |\vec{r}'\rangle, \quad (24)$$

let's denote the corresponding matrix element of an operator O by:

$$O^{\psi', \psi} := \langle \psi' | O | \psi \rangle. \quad (25)$$

For the results presented in this work we need the following operators.

The free boson Hamiltonian is diagonal:

$$H_{\text{FBD}}^{\psi', \psi} = \frac{\pi}{L} \left(\frac{R^2 m^2}{2} + \sum_{k=1}^{\infty} k r_k - \frac{1}{24} \right) \delta_{\psi', \psi}. \quad (26)$$

The Hamiltonian of the massive free boson:

$$H_{\text{mFBD}} = \frac{1}{8\pi} \int_0^L dx \left[(\partial_t \varphi)^2 + (\partial_x \varphi)^2 + m^2 \varphi^2 \right]. \quad (27)$$

has the following matrix elements:

$$H_{\text{FBD}}^{\psi',\psi} = \frac{\pi}{L} \left\{ \delta_{\psi',\psi} \left(\sum_{k=1}^{\infty} \left(1 + \frac{\tilde{m}^2}{2\pi^2 k^2} \right) kr_k - \frac{1}{24} \right) + \right. \\ \left. + \frac{\tilde{m}^2}{4\pi^2} \sum_{k=1}^{\infty} \left(\prod_{\substack{n=1 \\ n \neq k}}^{\infty} \delta_{r'_n, r_n} \right) \cdot \frac{1}{k^2} \left(\sqrt{r_k k} \sqrt{(r_k - 1)k} \delta_{r'_k + 2, r_k} e^{-i2\frac{\pi}{L}kt} + \sqrt{(r_k + 2)k} \sqrt{(r_k + 1)k} \delta_{r'_k - 2, r_k} e^{i2\frac{\pi}{L}kt} \right) \right\}, \quad (28)$$

where we have denoted by $\tilde{m} := mL$ the volume of the massive free boson.

The expression for a regularized vertex operator is:

$$V_n(z, \bar{z}) = e^{iq\varphi(z, \bar{z})} = |z - \bar{z}|^{-q^2} : e^{iq\varphi(z, \bar{z})} :. \quad (29)$$

Its matrix elements are:

$$V_n^{\psi',\psi} (e^{i\frac{\pi}{L}x}, e^{-i\frac{\pi}{L}x}) = N_{r'}^{-1} N_{\bar{r}}^{-1} \left[2 \sin \left(\frac{\pi x}{L} \right) \right]^{-q^2} \prod_{k=1}^{\infty} \langle 0 | a_k^{r'_k} e^{-q \frac{a_k}{k} (z^k - \bar{z}^k)} e^{q \frac{a_k}{k} (z^{-k} - \bar{z}^{-k})} a_{-k}^{r_k} | 0 \rangle, \quad (30)$$

with:

$$\langle 0 | a_k^{r'_k} e^{-q \frac{a_k}{k} (z^k - \bar{z}^k)} e^{q \frac{a_k}{k} (z^{-k} - \bar{z}^{-k})} a_{-k}^{r_k} | 0 \rangle = \\ = \sum_{j'=0}^{\infty} \sum_{j=0}^{\infty} \frac{1}{j'! j!} \left(\frac{2q}{k} \right)^{j'+j} \left[\frac{\bar{z}^k - z^k}{2} \right]^{j'+j} \langle 0 | a_k^{r'_k} a_{-k}^{j'} a_k^j a_{-k}^{r_k} | 0 \rangle \quad (31)$$

and:

$$\langle 0 | a_k^{r'_k} a_{-k}^{j'} a_k^j a_{-k}^{r_k} | 0 \rangle = k^{j'+j} \binom{r'_k}{j'} \binom{r_k}{j} j'! j! (r_k - j)! k^{r_k - j} \delta_{r'_k - j', r_k - j} \Theta(r_k \geq j). \quad (32)$$

To get the matrix elements of the integrated vertex operator that appears in the sine-Gordon Hamiltonian, the following relation is useful:

$$\int_0^{\pi} du [2 \sin(u)]^{-q^2} e^{-i(k+2qRm)u} = \frac{e^{-i\frac{\pi}{2}(k+2qRm)\pi}}{(1-q^2)B\left(\frac{1}{2}(2-q^2-k-2qRm), \frac{1}{2}(2-q^2+k+2qRm)\right)}. \quad (33)$$

Here, $B(x, y) = \frac{\Gamma(x)\Gamma(y)}{\Gamma(x+y)}$ is the beta function.

Lastly the matrix elements of the φ operator are:

$$\varphi^{\psi',\psi}(x, t) = 2\delta_{m',m} \sum_{n=1}^{\infty} \left(\prod_{\substack{k=1 \\ k \neq n}}^{\infty} \delta_{r'_k, r_k} \right) \left(\sqrt{\frac{r_n}{n}} \delta_{r'_n + 1, r_n} e^{-in\frac{\pi}{L}t} + \sqrt{\frac{r_n + 1}{n}} \delta_{r'_n - 1, r_n} e^{in\frac{\pi}{L}t} \right) \sin(n\frac{\pi}{L}x). \quad (34)$$

Thermal states and time evolution - To get thermal states, we compute the TCSA Hamiltonian in the regime of interest and compute the density matrix using numerical exponentiation:

$$\rho(H, \beta_T) = \frac{e^{-\beta_T H}}{\text{tr}(e^{-\beta_T H})}, \quad (35)$$

where $\beta_T = \frac{1}{T}$ is the inverse temperature and subscript T is used to distinguish it from the sine-Gordon coupling β .

Time evolution is computed by numerical exponentiation of the Hamiltonian:

$$U(H, t) = e^{-itH}. \quad (36)$$

Cutoff and truncation effects

The TCSA simulation is done by representing the operators as numerical matrices (using the matrix elements computed above) and introducing a cutoff. This is done by keeping only those states in the Hilbert space whose energy (with respect to the free boson Hamiltonian (26)) is below the chosen cutoff value. In this way we keep the matrices finite. The number of states in the Hilbert state for a chosen cutoff:

$$\text{cutoff} := (kr_k)_{\max} \quad (37)$$

is given by the cumulative sum of the (combinatorial) partition function:

$$\#\text{states} = \sum_{n=0}^{\text{cutoff}} p(n). \quad (38)$$

The values relevant for this work are listed in the table I.

cutoff	#states
15	684
16	915
17	1212
18	1597
19	2087
20	2714
21	3506
22	4508

Table I. Number of states in the Hilbert space for the energy cutoff values used in the paper.

The error emerging from the truncation is a systematic one and cannot be quantified statistically. However, there are several ways to determine the quality of the result and the parameter ranges where the method is reliable.

Note that truncation effects originate from neglecting the contribution of modes above the cutoff energy. Taking the states used in our computations and expanding them in the free boson basis one can examine the amplitudes versus the energies of the basis states, and check whether they decrease to a sufficiently small value for states in the vicinity of the cut-off. Another way to verify the results is to plot the values of the observables (for example correlation function time-series) for different values of the cutoff and check that they have converged. In our computation both approaches gave the same results, and using them we checked that the TCSA was reliable for all observables and parameter values used in this work.

Additionally we performed a number of nontrivial tests of our numerics through comparison with known analytical results and with other numerical methods. First, we compared the TCSA energy spectrum with that predicted by integrability following the approach in [47]. Second, we compared the expectation value of the vertex one-point function $\langle \cos \beta \phi \rangle$ to integrability predictions. We computed this value at the middle of the box with Dirichlet boundary conditions for various values of the interaction β using the TCSA. For the ground state in an infinite size system, an analytical formula by Lukyanov-Zamolodchikov [23] is available. For the ground state value in a finite box with periodic boundary conditions one can use numerical data from the so-called Non-Linear Integral Equation [55, 56]. In Fig. 7 we plot together the results for these three different types of states as functions of the interaction. TCSA data converge well for all values of interaction $\beta \lesssim 1.2$ ($\Delta \lesssim 0.055$), while the NLIE converges for $\beta \gtrsim 0.6$. In the region where the correlation length is small enough compared to the system size so that finite size and boundary effects are negligible, all three methods give results that agree with each other very well.

Correlation functions

As explained in the main text, multi-point correlation functions provide important physical information for a quantum field theory. In this work we are computing two- and four-point ($N = 2, 4$) equal-time correlation functions:

$$G^{(N)}(x_1, x_2, \dots, x_N)(t) = \langle \varphi(x_1, t) \varphi(x_2, t) \cdots \varphi(x_N, t) \rangle \quad (39)$$

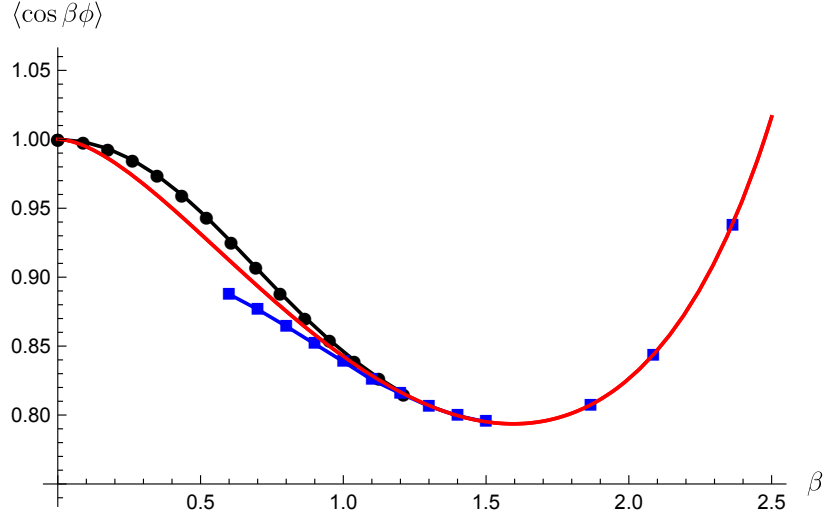


Figure 7. Comparison of $\langle \cos \beta \phi \rangle$ as a function of interaction β for three different types of states, computed by different methods: ground state in thermodynamically large system (red line) as given by the exact analytical formula of Lukyanov-Zamolodchikov [23], ground state in a finite system of length $L = 25$ with Dirichlet boundary conditions (black line and dots) computed from TCSA, ground state in a finite system of the same length with periodic boundary conditions (blue line and dots) computed numerically using the Non-Linear Integral Equation (NLIE) [55, 56]. The TCSA method gives reliable data for $\beta \lesssim 1.2$, while the NLIE method for $\beta \gtrsim 0.6$. The three lines converge for $\beta \gtrsim 1$ ($\Delta \gtrsim 0.04$), because for such interactions the mass of the lightest breather is sufficiently larger than (at least 3 times) the inverse system size, so that the system is practically in the thermodynamic limit (finite size effects and dependence on boundary conditions is negligible). This convergence provides a nontrivial verification for our numerics.

At equilibrium states of the SGM all the odd ($N = \text{odd}$) correlation functions vanish, since the field (17) is odd under reflection ($\varphi(x, t) = -\varphi(-x, t)$) and the SGM Hamiltonian (1) is even ($H(\varphi) = H(-\varphi)$).

The correlation functions are computed either in pure states $|\Psi\rangle$ (ground or excited states), in which case:

$$\langle O(t) \rangle = \langle \Psi | U(-t) O U(t) | \Psi \rangle, \quad (40)$$

or in mixed states (thermal states), in which case:

$$\langle O(t) \rangle = \text{tr} (U(-t) \rho U(t) O). \quad (41)$$

Connected correlation functions - If we are interested in studying only the genuine N -body interactions (N -particle collisions), we have to subtract from the full correlation function $G^{(N)}$ the contributions that come from lower order correlation functions (fewer particle collisions). One gets what is called the connected part of the correlation functions, which are essentially the joint cumulants of the fields in the state under consideration

$$G_{\text{con}}^{(N)}(x_1, x_2, \dots, x_N) = \sum_{\pi} \left[(|\pi| - 1)! (-1)^{|\pi|-1} \prod_{B \in \pi} \left\langle \prod_{i \in B} \varphi(x_i) \right\rangle \right]. \quad (42)$$

Here, π are all possible partitions of $\{1, 2, \dots, n\}$ into blocks B and i are elements of B . $|\pi|$ is the number of blocks in the partition. All the correlation functions can be taken at time t .

In case of four-point functions and vanishing odd correlation functions, this formula simplifies to:

$$G_{\text{con}}^{(4)}(x_1, x_2, x_3, x_4) = G^{(4)}(x_1, x_2, x_3, x_4) - \\ - G^{(2)}(x_1, x_2) G^{(2)}(x_3, x_4) - G^{(2)}(x_1, x_3) G^{(2)}(x_2, x_4) - G^{(2)}(x_1, x_4) G^{(2)}(x_2, x_3). \quad (43)$$

Kurtosis - To estimate how close the states are to Gaussian, that is, to see the strength of interaction effects, we compute the kurtosis, that is the ratio between the integrated connected and full four-point correlation function [2]:

$$\mathcal{K} := \frac{\int dx_1 dx_2 dx_3 dx_4 |G_{\text{con}}^{(4)}(x_1, x_2, x_3, x_4)|}{\int dx_1 dx_2 dx_3 dx_4 |G^{(4)}(x_1, x_2, x_3, x_4)|} \approx \frac{\sum_{x_1, x_2, x_3, x_4} |G_{\text{con}}^{(4)}(x_1, x_2, x_3, x_4)|}{\sum_{x_1, x_2, x_3, x_4} |G^{(4)}(x_1, x_2, x_3, x_4)|}, \quad (44)$$

where in the last equality we used that in the numerical simulation the domain is discretized so the integral is approximated with a sum. For Gaussian states, \mathcal{K} vanishes, while a larger value of \mathcal{K} corresponds to a more strongly interacting system.

For the evaluation of the kurtosis one needs the 4-p correlated functions over the entire four dimensional grid of spatial positions. However, using the full grid is computationally expensive, so for quench time sequences we used a random sampling method over a thousand points, checking at a few time slices that it correctly reproduces the kurtosis result obtained from the full grid. For the initial state of the quench, and for equilibrium states we always used the full computation.

Quench from a ground state

In this section we present an interaction quench starting from the ground state of the SGM for $\Delta_0 = 1/9$ to $\Delta = 1/8$ which is shown in Fig. 8. Note the almost complete absence of 4-p connected correlations, which is due to the energy density of the post-quench system being negligible compared to the height of the cosine potential. In contrast to the case of quench starting from an excited initial state, studied in the main text, in the present case the quench dynamics is dominated by low energy modes, the leading one being the lowest lying second breather mode (due to parity invariance the odd states do not contribute).

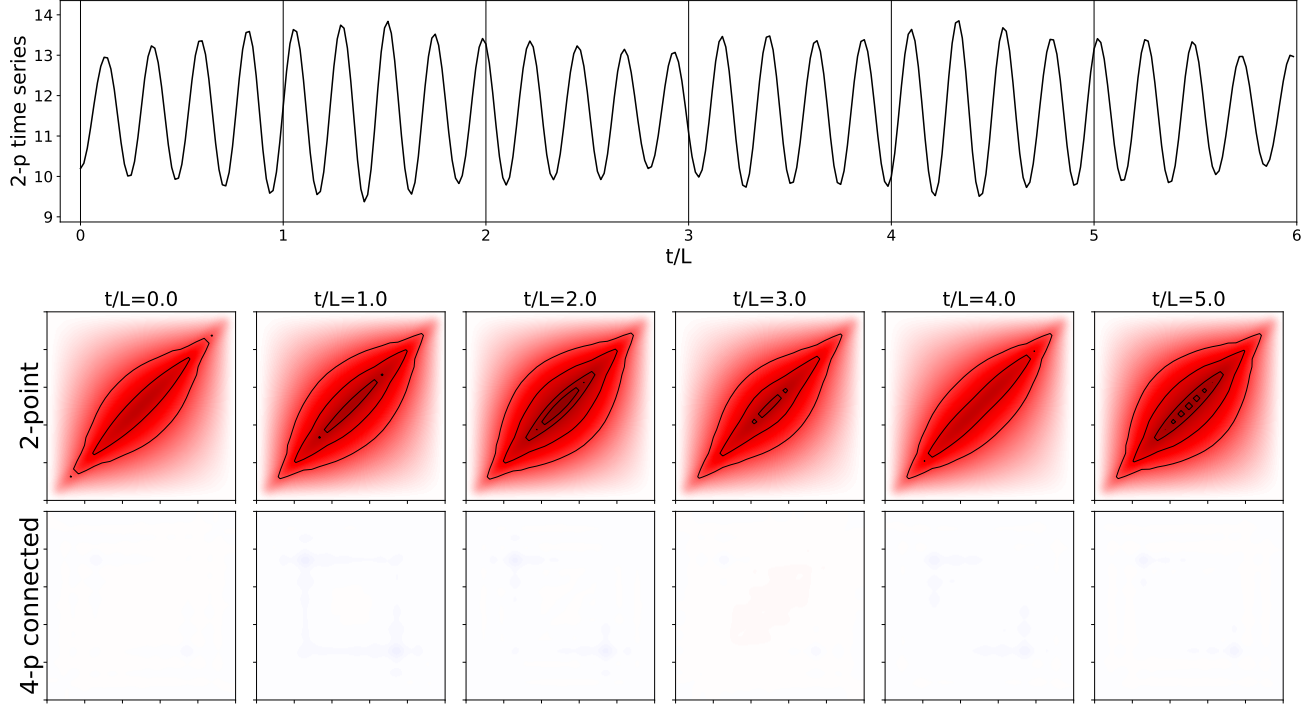


Figure 8. Time evolution of 2-p correlations $G^{(2)}(L/3, 2L/3; t)$ (top) and spatial density plots of 2-p correlations $G^{(2)}(x_1, x_2; t)$ and 4-p correlations $G^{(4)}(x_1, x_2, L/4, 3L/4; t)$ at various times t (bottom two rows) after a quench starting from a ground state of the SGM (pre-quench interaction: $\Delta_0 = 1/9$, post-quench interaction: $\Delta = 1/8$, $L = 30/M$).

The Fourier spectrum of the time evolution of observables is determined by the post-quench excitations, which are multi-particle states with momenta quantised by the finite box. The complete set of equations that determine the energy levels can be found e.g. in [47]. Here we focus only on the dominant energy level which corresponds to the $n = 2$ breather moving with the lowest momentum $p(\theta) := m_2 \sinh \theta$ allowed by the Bethe Yang equations:

$$e^{2ip(\theta)L} R(\theta)^2 = +1 \quad (45)$$

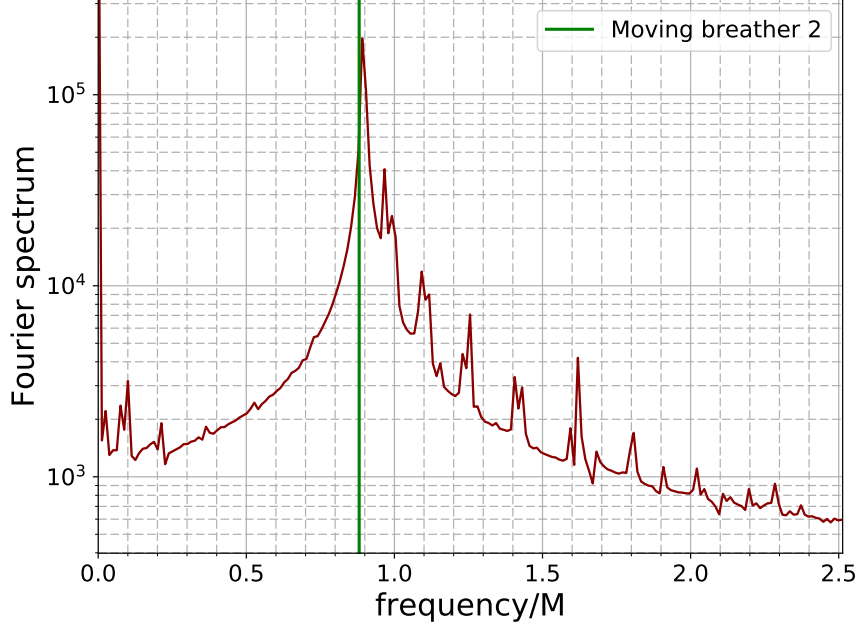


Figure 9. Fourier spectrum of the time dependence of the spatially integrated 2-p correlations after the ground state quench shown in Fig. 8.

where the second breather reflection factor for Dirichlet boundary conditions is [45, 57]:

$$R(\theta) = \frac{\left(\frac{1}{2}\right)_\theta \left(1 + \frac{\xi}{2}\right)_\theta \left(\frac{\xi}{2}\right)_\theta \left(1 + \xi\right)_\theta}{\left(\frac{1}{2} + \frac{\xi}{2}\right)_\theta^2 \left(\frac{1}{2} - \frac{\xi}{2}\right)_\theta^2 \left(\frac{3}{2} + \xi\right)_\theta \left(\frac{3}{2} + \frac{\xi}{2}\right)_\theta^2} \quad (46)$$

and the notation

$$(x)_\theta := \frac{\sinh\left(\frac{\theta}{2} + \frac{i\pi x}{2}\right)}{\sinh\left(\frac{\theta}{2} - \frac{i\pi x}{2}\right)} \quad (47)$$

has been used. Note that static breathers are not present for Dirichlet boundary conditions. From these equations we find that the energy of this mode measured from the ground state is $E = 0.881039M$, which matches with the frequency of the dominant peak in the Fourier spectrum of 2-p correlations, shown in Fig. 9.